The Aguablanca Cu–Ni ore deposit (Extremadura, Spain), a case of synorogenic orthomagmatic mineralization: age and isotope composition of magmas (Sr, Nd) and ore (S)

C. Casquet [a,*], C. Galindo [a], F. Tornos [b], F. Velasco [c], A. Canales [d]

[a] *Departamento de Petrología y Geoquímica, Facultad de Geología, Universidad Complutense, 28040 Madrid, Spain*
[b] *Instituto Tecnológico Geominero de España, Rios Rosas 23, 28003 Madrid, Spain*
[c] *Departamento de Mineralogía y Petrología, Universidad País Vasco, Apdo 644, 48080 Bilbao, Spain*
[d] *PRESUR, 21279 Minas de Cala, Huelva, Spain*

Abstract

The Aguablanca Cu–Ni orthomagmatic ore deposit is hosted by mafic and ultramafic rocks of the Aguablanca stock, which is part of the larger, high-K calc-alkaline Santa Olalla plutonic complex. This intrusive complex, ca. 338 Ma in age, is located in the Ossa-Morena Zone (OMZ) of the Iberian Variscan Belt. Mineralization consists mainly of pyrrhotite, pentlandite and chalcopyrite resulting from the crystallization of an immiscible sulphide-rich liquid. Isotope work on the host igneous rocks (Sr, Nd) and the ore (S) suggests that contamination with an upper-crustal component took place at some depth before final emplacement of the plutons ($\varepsilon Nd_{338} = -6$ to -7.5; $Sr_{(338)} = 0.7082$ to 0.7100; $\delta^{34}S_{(sulphides)}$ near $+7.4‰$). Assimilation–fractional crystallization (AFC) processes are invoked to explain early cumulates and immiscible sulphide-magma formation. Intrusion took place at the beginning of the type-A oblique subduction of the South Portuguese Zone under the Ossa-Morena Zone and was probably driven by transpressive structures (strike-slip faults). The mineralization is thus synorogenic.

Aguablanca is probably the first case referred to in the literature of a magmatic Cu–Ni ore deposit hosted by calc-alkaline igneous rocks.

Keywords: Cu–Ni ores; Calc-alkaline magmatism; Isotope geochemistry; Variscan orogeny; Spain

1. Introduction

The Aguablanca Cu–Ni ore is an orthomagmatic sulphide deposit hosted by mafic and ultramafic rocks of the Aguablanca stock, which is part of the Santa Olalla plutonic complex in SW Spain (Fig. 1). This complex is a K_2O-rich calc-alkaline composite intrusion formed mainly of gabbronorite and norite, diorite, tonalite and monzogranite. The deposit was discovered after a regional geochemical prospection survey. Geological resources are 30–35 Mt with 0.6–0.75 wt.% Ni, 0.5–0.6 wt.% Cu and minor amounts of Co (0.02 wt.%), Pt (0.3 ppm), Pd (0.3 ppm) and Au (0.15 ppm) (Ortega et al., 1999).

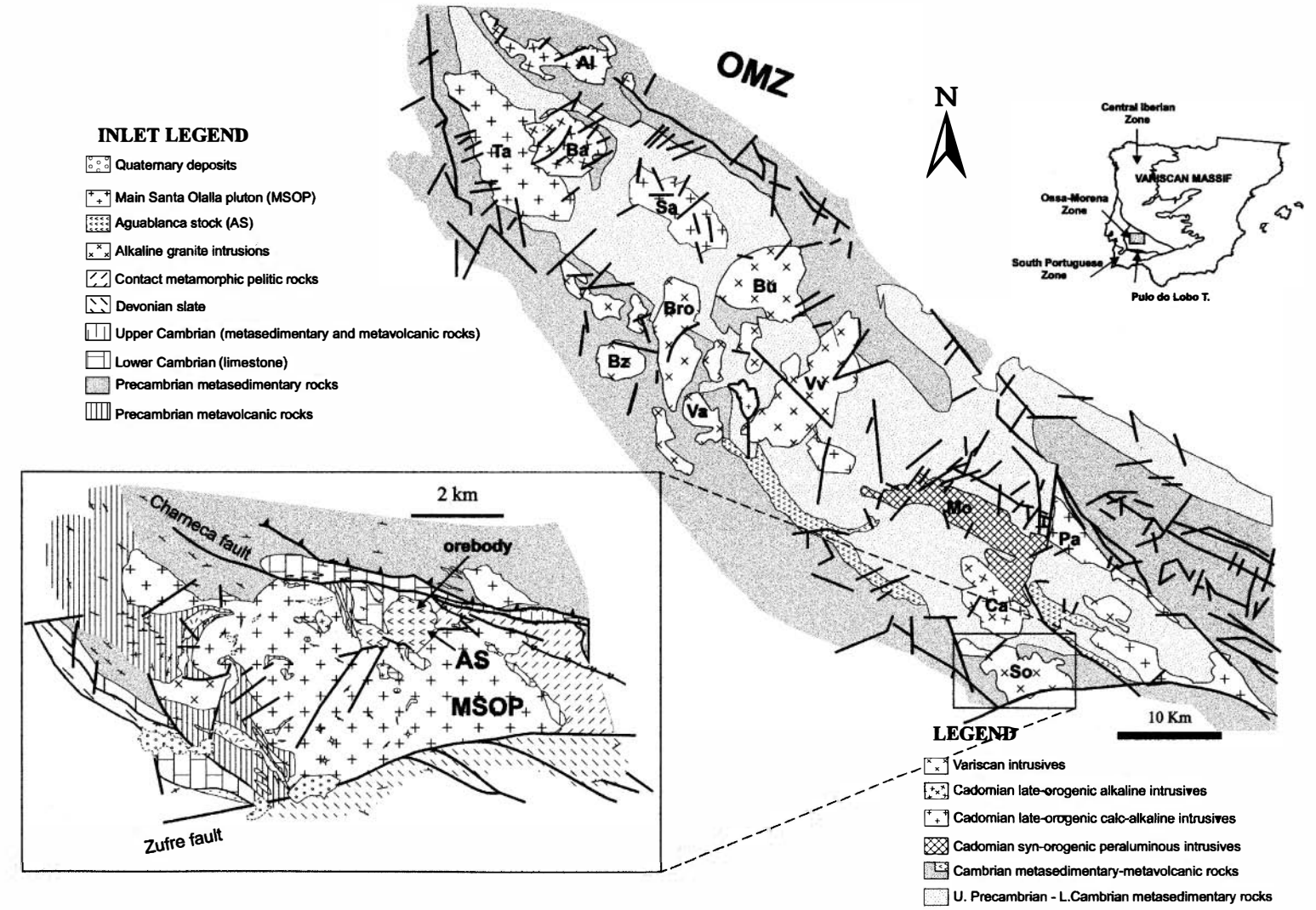

Fig. 1. Geological map of the Santa Olalla plutonic complex and location within the Monesterio Antiform. Plutonic massifs: Al: Almendral; Ta: Táliga; Ba: Barcarrota; Sa: Salvatierrra; Bu: Burguillos; Bro: Brovales; Bz: Bazana, Va: Valuengo; Vv: Valencia el Ventoso; Mo: Monesterio; Pa: Pallarés; So: Santa Olalla. Inset shows an enlargement of the Santa Olalla plutonic complex and ore deposit location.

This is the first ore deposit of its type to be found in Spain and is unique in the European Union.

A first study of the igneous rocks was carried out by Casquet (1980), prior to the discovery of the ore deposit. In this contribution, we provide new geochemical evidence (trace elements and rare earths, and stable (S) and radiogenic isotopes (Sr and Nd)) that shed new light on the source and evolution of the magmas and ore. Moreover, we argue that the emplacement of the magmas and ore was synorogenic.

Most synorogenic Cu–Ni deposits are small and hosted by Alaskan-type mafic–ultramafic plutonic complexes (Naldrett, 1989a). The Santa Olalla ore is a special case of a Cu–Ni deposit inasmuch as it is hosted by a K_2O-rich calc-alkaline intrusive complex, something which has not been reported before, to our knowledge.

2. Geological setting

The Santa Olalla plutonic complex was emplaced in the southern limb of the large Monesterio antiform, into low-grade metavolcanic and metasedimentary rocks (metapelites, marbles and calc-silicate rocks) of Upper Precambrian–Lower Cambrian age. To the south it ends abruptly against the Zufre fault (Fig. 1). Regional cleavage and bedding generally wrap around the intrusive massif. However, in detail, discordant contacts are common, suggesting that an earlier stage of forceful intrusion was followed by stoping. The stoping process is evidenced by the abundance of roof pendants in the central part of the massif. A well-developed contact metamorphic aureole encircles the Santa Olalla plutonic complex, with temperatures reaching hypersthene hornfels facies conditions (700–750 °C). Partial melting of pelitic hornfelses has locally been recorded (nebulites and heterogeneous migmatites). Skarns are also abundant within the aureole. Probable emplacement depth was 2–4 km (0.5–1 kb) (Casquet, 1980). The Santa Olalla plutonic complex is one of a series of Variscan massifs of similar characteristics extending into nearby Portugal (see Fig. 1).

The Monesterio antiform is part of the Ossa-Morena Zone (OMZ), which is one of the subdivisions of the Variscan Iberian Massif (Fig. 1). The OMZ is a complex terrane consisting of an Upper Proterozoic–Lower Palaeozoic Cadomian basement, reworked during the Variscan Orogeny. The geodynamic evolution of this part of the Variscan Iberian Massif has been the subject of many reviews (Silva et al., 1990, among others).

We address here the Variscan part of the evolution of the OMZ pertinent to the tectonic setting of the ore deposit. There is a consensus that deformation resulted from north-verging oblique subduction and the amalgamation of two different terranes to the southern margin of the OMZ. The first of these is the Pulo de Lobo Terrane, together with the allied Beja Ophiolite, derived from the partial obduction of a pre-Famennian oceanic basin. The other terrane is the South Portuguese Zone, which hosts the famous Iberian Pyrite Belt, consisting of massive sulphide (VHMS) deposits.

Subduction of oceanic crust beneath the OMZ took place from the Middle-Upper Devonian to the Lower Carboniferous (Visean), with the situation merging into type-A oblique subduction (thrusting of the SPZ under the OMZ) during the Upper Visean to Middle Westphalian interval (Silva et al., 1990).

3. The igneous rocks

The Santa Olalla plutonic complex consists of two larger plutons, the main Santa Olalla pluton and the Aguablanca stock, as well as felsic dykes (Fig. 1).

The main Santa Olalla pluton is the largest intrusion. Reverse compositional zoning of the pluton is remarkable, with amphibole-biotite quartz diorites merging into tonalites, and these in turn into monzogranites, towards the centre of the pluton (Velasco, 1976; Casquet, 1980). The transitions between the igneous types are gradational. The Aguablanca stock is a small (less than 3 km^2), mafic–ultramafic, relatively older intrusion in the northern part of the complex that shows a discontinuous outer zone of pyroxene-rich rocks (PG rocks in Table 2), largely biotite-bearing melanocratic hornblende gabbronorites and biotite-bearing hornblende norites, and an inner zone of clinopyroxene-bearing biotite-amphibole diorites and quartz-diorites. The first rocks

Table 1
Chemical analyses of representative samples of the Santa Olalla plutonic complex

Sample	Aguablanca stock						Santa Olalla pluton				
	C3	C19	C23	C4	C21	C22	C2	C10	C16	C15	C14
	PG	PG	PG	DI	DI	DI	DI	TO	TO	TO	MO
SiO_2	48.40	56.50	53.25	55.60	56.00	55.60	56.60	59.00	60.00	61.10	67.80
Al_2O_3	12.75	10.75	13.57	16.57	14.08	14.60	18.35	16.44	16.91	16.15	15.44
Fe_2O_3	1.87	1.25	1.61	1.84	1.15	0.79	1.39	1.63	2.06	1.78	2.04
FeO	7.08	6.33	5.65	5.34	7.05	6.56	5.29	4.62	3.62	3.96	1.85
MnO	0.16	0.14	0.14	0.11	0.16	0.12	0.10	0.10	0.09	0.07	0.03
MgO	16.23	12.62	12.24	6.65	6.89	5.93	4.23	4.78	3.79	3.63	0.89
CaO	7.71	8.29	9.10	5.89	6.69	7.49	5.05	5.05	5.55	4.91	2.63
Na_2O	2.16	1.67	2.00	3.67	2.80	3.88	3.99	3.24	3.13	2.70	3.07
K_2O	0.58	0.67	0.58	2.22	2.02	1.35	2.65	2.46	2.16	2.41	4.62
TiO_2	0.52	0.42	0.47	0.88	0.82	0.91	0.98	0.78	0.83	0.90	0.51
P_2O_5	0.20	0.08	0.33	0.21	0.47	0.29	0.34	0.17	0.27	0.25	0.13
SO_3	0.30	0.00	0.00	0.00	0.00	0.00	0.00	0.00	0.00	0.00	0.00
CO_2	0.00	0.00	0.00	0.00	0.00	0.00	0.00	0.13	0.00	0.00	0.00
Cl	0.00	0.00	0.00	0.00	0.00	0.00	0.00	0.00	0.00	0.00	0.00
H_2O	2.03	1.07	0.91	0.96	1.80	2.20	1.01	1.35	1.55	1.78	1.14
Total	99.99	99.79	99.85	99.94	99.93	99.72	99.98	99.75	99.96	99.64	100.15
Rb	16.5	26.9	17.6	89.7	73.6	37.5	92.5	85.9	85.7	99.7	121
Sr	235	266	311	299	316	281	315	325	356	299	225
Ba	423	171	462	746	954	n.d.	852	475	645	559	1368
Cr	1200	837	738	285	8.9	n.d.	145	141	120.0	124	17.5
Co	74.7	57.0	57.3	135	55.0	61.0	125	24.0	25.0	27.0	7.94
Ni	515	351	317	132	168	169	60.5	87	62.0	64.0	9.52
Cu	109	24.0	10	66.9	8.0	123	52.3	7.00	29.0	15.0	4.63
Zn	89.7	45.0	117	74.8	61.0	40.0	59.7	38.0	77.0	76.0	18.2
Y	12.9	12.3	10.4	28.8	32	n.d.	25.0	21.9	24.4	21.6	29.6
Nb	3.53	3.04	4.34	16.2	20.6	n.d.	21.1	11.6	14.3	12.5	20.0
Zr	111	57	64.9	243	81	58	173	109	177	240	261
Th	1.79	2.34	1.81	9.13	12.8	n.d.	3.89	8.28	10.1	10.9	10.3
Ta	1.20	0.34	2.10	4.90	1.44	n.d.	4.90	0.91	0.95	0.88	2.60
Hf	2.1	0.79	1.3	4.8	5.55	n.d.	2.90	1.33	1.24	1.46	5.60
La	10.45		8.92	34.09			33.26				33.25
Ce	21.04		18.18	70.52			71.28				83.64
Pr	2.56		2.11	8.30			8.61				7.65
Nd	10.47	9.36	8.59	28.27	24.33	20.30	28.97	24.50	28.80	32.03	37.87
Sm	2.42	2.30	1.99	5.90	5.54	4.30	5.96	5.06	5.91	6.00	7.45
Eu	0.76		0.77	1.52			2.00				1.58
Gd	2.74		2.12	7.44			7.70				7.11
Tb	0.40		0.34	1.05			1.04				0.96
Dy	2.35		1.98	5.62			5.21				5.36
Ho	0.47		0.39	1.11			0.98				1.05
Er	1.44		1.16	3.26			2.77				3.10
Tm	0.19		0.17	0.46			0.38				0.45
Yb	1.32		1.08	2.99			2.31				2.93
Lu	0.19		0.18	0.43			0.33				0.43
ΣREE	57		48	171			171				193

PG = gabbro-norites and norites; DI = diorites; TO = tonalites; MO = monzogranite. Major elements are from Casquet (1980). Trace elements were determined at Actlabs (Canada).

consist for the most part of idiomorphic orthopyroxene and to a lesser extent clinopyroxene, with the OPX/CPX ratio increasing towards the noritic terms. Plagioclase, hornblende and biotite are interstitial phases. Minor idiomorphic olivine crystals can be found in the most basic types and allotriomorphic quartz in the more acidic varieties. These rocks are interpreted as pyroxene cumulates and they host the main sulphide mineralization. Enclaves of skarns and micro-enclaves of peraluminous composition are occasionally found in the mafic–ultramafic rocks. The latter enclaves consist of plagioclase, biotite, hercynite, corundum and sillimanite. Very small bodies of fine-grained porphyritic quartz-biotite norites and orthopyroxene-biotite microgranites have also been found transecting the Aguablanca diorites.

3.1. Geochemical features

Chemically, two main groups of rocks can be distinguished in the Santa Olalla plutonic complex: the noritic and gabbronoritic cumulates of the Aguablanca stock, and the main igneous sequence that includes the rest of the Aguablanca stock rocks and the main Santa Olalla pluton rocks (Table 1; Figs. 2 and 3). The cumulates (samples C3, C19 and C23) show SiO_2 contents of 48–57 wt.% and are relatively low in K_2O (< 0.7 wt.%) and incompatible trace elements (Ba, Rb, Th, Nb). Furthermore, they show high contents of MgO (12.2–16.2 wt.%), Ni (317–515 ppm) and Cr (738–1200 ppm). Total REE contents are low (48–57 ppm); chondrite-normalized patterns show moderate enrichment of LREEs ($(La/Lu)_N$ = 11.4–12.3)) and small Eu anomalies (Eu/Eu^* = 0.9–1.1). The main igneous sequence consists of metaluminous Hy + Q normative rocks with SiO_2 contents of 55.6–67.8 wt.% and K_2O values of up to 4.6 wt.%. These rocks form regular "differentation" arrays on classic Harker plots (e.g., Fig. 2b). LIL elements (Ba, Rb), as well as Th and to a lesser extent Ce, are enriched in main igneous sequence rocks. The ranges of Rb and Sr contents in the main igneous sequence are 37.5–121 ppm and 225–356 ppm, respectively. On the other hand, Nb shows significant depletion. REE element patterns display enrichment in LREE ($(La/Lu)_N$ = 17.2–22.8) and a small negative Eu anomaly (Eu/Eu^* = 0.7). Total REE contents increase from the diorites towards monzogranite. The main igneous sequence is a K_2O-rich calc-alkaline association, as evidenced in SiO_2–K_2O and AFM plots (Fig. 2).

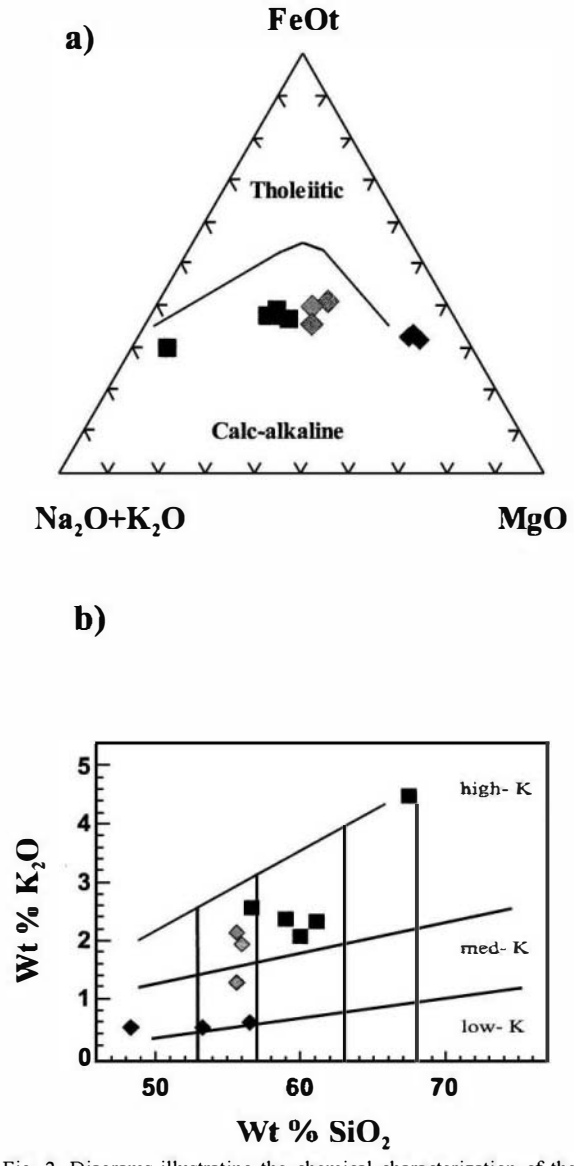

Fig. 2. Diagrams illustrating the chemical characterization of the Santa Olalla igneous rocks (Wilson, 1989): (a) $Na_2O + K_2O$–FeO_t–MgO triangular diagram with tholeiitic and calc-alkaline fields outlined, and (b) K_2O vs. SiO_2 diagram showing calc-alkaline sub-series. Squares: Santa Olalla pluton; diamonds: Aguablanca stock (black = PG rocks; grey = diorites).

4. The ore

The deposit is a lens-shaped breccia-pipe, about 500-m long, 60–100-m wide, and more than 700-m deep (Tornos et al., 1999). It dips steeply (70°S) and is found a few tens of metres from the northern contact of the Aguablanca stock and close to an important fault, the Cherneca fault (Fig. 1). At this locality, the pluton host rocks are marbles and calc-silicate hornfelses, overprinted by a Ca-skarn consisting of wollastonite, garnet, clinopyroxene and scapolite. This skarn is not mineralized. Moreover, enclaves of the skarn are found within the Aguablanca stock, suggesting that the skarn formed before the crystallization of the igneous rocks (Casquet, 1980).

The mineralized breccia-pipe consists of rounded and subangular fragments of ore-bearing or barren igneous rocks, including gabbros, pyroxenites, both orthopyroxene- and clinopyroxene-rich varieties, and a very minor, completely serpentinized rock, probably peridotite. The ore fills the spaces between fragments. The mineralization consists mainly of pyrrhotite, pentlandite and chalcopyrite (Tornos et al., 1999). Textural evidence from the massive ore suggests that several stages of mineral formation were involved in the formation of this ore deposit. (1) The first, probably the consequence of the crystallization of an immiscible sulphide-rich liquid, gave rise to massive, coarse-grained (0.2–3 mm) pyrrhotite with fine (50–100 μm), flame-like exsolutions of pentlandite ($Ni_{0.31}Fe_{0.27}S_{0.45}$) and chalcopyrite intergrowths with minor cubanite and magnetite. Sulphides are interstitial to idiomorphic cumulus crystals of orthopyroxene and clinopyroxene. (2) A second stage is evidenced by a new generation of coarse-grained recrystallized pyrrhotite, chalcopyrite and pentlandite ($Ni_{0.24}Fe_{0.25}S_{0.51}$) that replace the earlier sulphides. Minor amounts of mackinawite, rutile and cobaltite also formed during this stage. (3) A third stage is represented by the transformation of pentlandite to violarite along grain boundaries and fractures, and the growth of pyrite and new chalcopyrite and pyrrhotite. Finally, marcasite formed as late replacements of pyrite and pyrrhotite (Tornos et al., 1999).

Igneous fragments in the breccia-pipe show low-temperature hydrothermal alteration, probably coincident with the formation of postmagmatic sulphides. Minerals such as biotite, actinolite, epidote, sericite, talc, serpentine, chlorite and clay minerals formed at the expense of pyroxenes and olivine.

Lunar et al. (1997) and Ortega et al. (1999) first described Pt-group minerals in the Aguablanca ore deposit. These minerals are Pd and Pd–Pt-tellurides such as michenerite, merenskyte, palladium melonite, and members of the solid solution merenskyte–moncheite. Sperrylite has also been found, as well as other minor phases such as tellurobismuthite, bismuthite, hessite, volynskyite, galena and native gold.

5. Isotope analytical work

Thirteen rocks were chosen for Rb–Sr and Sm–Nd determinations away from the mineralized breccia-pipe, where subsolidus alteration is larger, that showed minor amounts of chlorite, talc, calcite and uralite; the results are portrayed in Table 2. Analyses were carried out at the National Isotope Geosciences Laboratory (Keyworth, UK) and at the Geochronology and Isotope Geochemistry Centre of the Complutense University (Madrid, Spain). Errors are quoted throughout as two standard deviations from measured or calculated values. The decay constants used in the calculations are the values $\lambda^{87}Rb = 1.42 \times 10^{-11}$ and $\lambda^{147}Sm = 6.54 \times 10^{-12}$ year^{-1} recommended by the IUGS Subcommission for Geochronology (Steiger and Jäger 1977). Analytical uncertainties are estimated to be 0.01% for $^{87}Sr/^{86}Sr$ ratios and 0.006% for $^{143}Nd/^{144}Nd$ ratios and 1.0% and 0.1% for the $^{87}Rb/^{86}Sr$ and $^{147}Sm/^{144}Nd$ ratios, respectively. Epsilon-Nd (εNd) values (Jacobsen and Wasserburg, 1980) were calculated relative to a chondrite present-day $^{143}Nd/^{144}Nd$ value of 0.51262 and $^{147}Sm/^{144}Nd$ of 0.1967. Replicate analyses of the NBS-987 Sr-isotope standard yielded an average $^{87}Sr/^{86}Sr$ ratio of 0.710247 ± 0.000024 ($n = 215$). Fifty-six analyses of the Johnson and Matthey Nd-standard over 1 year gave a mean $^{143}Nd/^{144}Nd$ ratio of 0.511114 ± 0.000026.

In addition, 19 sulphur isotope determinations were made at the Salamanca University Isotope Laboratory (Spain) on sulphides, particularly chalcopyrite, pyrrhotite and pentlandite from the Aguablanca mineralization (Table 3).

Table 2
Rb–Sr and Sm–Nd isotope data of samples from the main Santa Olalla pluton and Aguablanca stock

Sample		Rb	Sr	Rb/Sr	$^{87}Rb/^{86}Sr$	$^{87}Sr/^{86}Sr$	$^{87}Sr/^{86}Sr_{333}$	εSr_{333}	Sm	Nd	$^{147}Sm/^{144}Nd$	$^{143}Nd/^{144}Nd$	$^{143}Nd/^{144}Nd_{333}$	εNd_{333}	TDM_{333}
Santa Olalla pluton															
C2	DI	92.5	315	0.2940	0.8511	0.713449	0.709354	75	5.96	28.97	0.1243	0.512121	0.511846	−7.0	1.64
C10	TO	85.9	325	0.2644	0.7654	0.713706	0.710024	84	5.06	24.50	0.1248	0.512097	0.511821	−7.5	1.67
C15	TO	99.7	299	0.3332	0.9646	0.714153	0.709512	77	6.00	32.03	0.1132	0.512149	0.511898	−6.0	1.56
C16	TO	85.7	356	0.2407	0.6967	0.712670	0.709318	74	5.91	28.80	0.1240	0.512110	0.511836	−7.2	1.65
C14	MO	121	225	0.5357	1.5514	0.717295	0.709831	81	7.45	37.87	0.1190	0.512091	0.511828	−7.4	1.66
Aguablanca stock															
C3	PG	16.5	235	0.0701	0.2028	0.709243	0.708267	59	2.42	10.47	0.1386	0.512244	0.511937	−5.2	1.51
C19	PG	26.9	266	0.1010	0.2923	0.709723	0.708317	60	2.30	9.36	0.1485	0.512218	0.511889	−6.2	1.58
C23	PG	17.6	311	0.0566	0.1638	0.709041	0.708253	59	1.99	8.59	0.1400	0.512202	0.511892	−6.1	1.58
C4	DI	89.7	299	0.3003	0.8693	0.713440	0.709258	73	5.90	28.27	0.1262	0.512137	0.511858	−6.8	1.63
C21	DI	73.6	316	0.2328	0.6739	0.712758	0.709516	77	5.54	24.33	0.1376	0.512140	0.511835	−7.2	1.66
C22	DI	37.5	281	0.1334	0.3861	0.710395	0.708537	63	4.30	20.30	0.1279	0.512175	0.511892	−6.1	1.58
Metamorphic and volcanic rocks															
DC4	MP	65.4	233	0.2807	0.8131	0.720221	0.716309	173	4.23	20.80	0.1229	0.511912	0.511640	−11.0	1.92
MON-4	MP	278	1866	0.1491	0.4319	0.716227	0.714149	143	4.78	25.50	0.1133	0.511756	0.511505	−13.7	2.09
CEM-113	V	4.64	123	0.0377	0.1093	0.704777	0.704251	2.20	9.75	46.60	0.1265	0.512654	0.512374	3.3	0.82

Rock type abbreviations as in Table 1. DC-4 and MON-4 are metasediments (MON-4 from Schäfer, 1990) and CEM-113 is a Middle Cambrian basalt.

Table 3
S-isotope composition of sulphides from the Aguablanca ore

Sample	Mineral	δ^{34}S‰
91	cpy	+7.43
	po	+7.45
92	po	+7.14
	py	+7.23
93	po	+7.20
	cpy	+7.33
94	po	+7.60
	cpy	+7.73
95	po	+7.11
	cpy	+7.24
100	po	+7.50
	cpy	+7.64
101	po	+7.49
	cpy	+7.63
102	po	+7.50
	cpy	+7.18
	plt	+7.38
103	po	+7.49
104	po	+7.75

cpy: chalcopyrite; po: pyrrhotite; py: pyrite; plt: pentlandite.

The Sr-isotope composition of the igneous rocks at a reference age of 338 Ma (see below) ranges from 0.7082 to 0.7100. Aguablanca cumulates show Sr_{338} values of 0.708253 to 0.708317, while the main igneous sequence rocks show slightly higher values (between 0.7085 and 0.7100, most rocks plotting in the range 0.7092–0.7095). The Nd-isotope composition, expressed as εNd_{338} values, ranges from −5.2 to −6.1 for the Aguablanca cumulates and −6 to −7.5 for the main igneous sequence rocks (Table 2). The isotope composition of sulphur in ore sulphides is very similar in all samples, with a mean close to +7.4 per mil ($\delta^{34}S_{cp}$ = +7.2‰ to +7.7‰; $\delta^{34}S_{po}$ = +7.1‰ to +7.8‰; $\delta^{34}S_{pent}$ = +7.4‰).

6. Interpretation and discussion

6.1. *Geochronology of the Santa Olalla plutonic complex*

The $^{87}Sr/^{86}Sr$–$^{87}Rb/^{86}Sr$ isochron plot of the main igneous sequence rocks yields an errorchron age of 359 ± 18 Ma, with a Mean Standard Weighted Deviation (MSWD) of 17.1. The resulting initial Sr-isotope composition is 0.7092 (Casquet et al., 1999). The large MSWD suggests that causes other than analytical error are probably involved in the dispersion of isotopic compositions, either primary compositional heterogeneity or secondary subsolidus alteration.

Radiometric evidence from nearby similar plutonic massifs can help to constrain the age of the Santa Olalla plutonic complex. Allanite from an Fe-U-REE skarn-type deposit at Mina Monchi, within the Burguillos del Cerro intrusive massif (Bu; Fig. 1), has given a concordia U–Pb age of 338 ± 1.5 Ma, i.e., Visean (Casquet et al., 1998). This value is in agreement with the $^{40}Ar/^{39}Ar$ ages of magmatic amphiboles from the same massif (Dallmeyer et al., 1995).

The age of the Burguillos allanite is taken here as the most probable age of the zoned metaluminous intrusive massifs and is almost within the error margin of the main igneous sequence Rb–Sr age referred to above.

6.2. *Source components of magmas*

The scattering of the K_2O values (Fig. 2b) is characteristic of high-K magmatism of active continental margins and is attributed to contamination with a crustal component (e.g., Wilson, 1989). The contents of trace elements are more indicative of the genesis than those of major element oxides. Fig. 3 shows the trace-element variation normalized to chondrite of the main igneous sequence rocks and cumulates. The average composition of the upper-continental crust has been added for comparison. Patterns from Ba to Ti depart from those of primitive magmas and are remarkably similar to the continental crust (Rollinson, 1993). The Nb negative anomaly is very significant in this respect. Furthermore, the enrichment in Rb and Th is characteristic of contamination with an upper-continental crust component (Wilson, 1989).

The radiogenic isotope evidence (high initial $^{87}Sr/^{86}Sr$ values and very negative εNd_{338} values) suggests the involvement of a component rich in radiogenic Sr and poor in LREE in the magma composition. Model ages ($T_{DM(338)}$) calculated using the method of Börg et al. (1990) range from 1.51 to

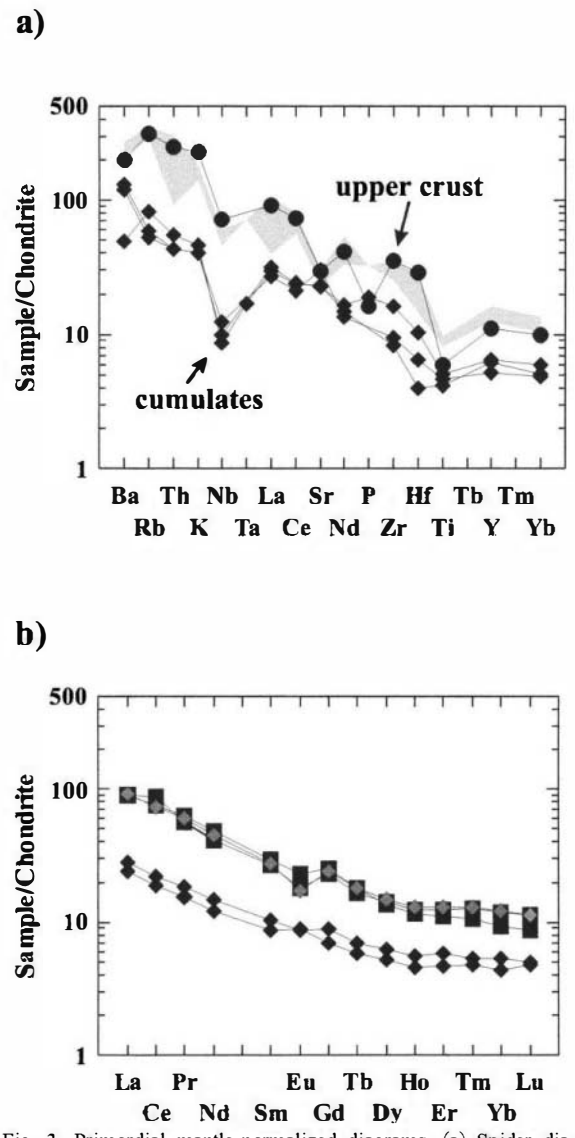

Fig. 3. Primordial mantle-normalized diagrams. (a) Spider diagram (after Thompson, 1982) of main igneous sequence rocks (shaded) and PG rocks (diamonds). Circles: upper-crust composition (after Taylor and McLennan, 1981), and (b) REE/chondrite (C1) normalized plot. Squares: Main Santa Olalla pluton. Diamonds: Aguablanca stock (black = PG rocks; grey = diorites).

1.67 Ga (Table 2). This range suggests that this component might have derived from a continental crust containing old resident Nd. The existence of a circa 2 Ga pre-Cadomian basement in the Ossa-Morena Zone has been convincingly argued for Nägler (1990) from Nd-isotope work on sedimentary rocks.

Fig. 4 is an εNd_{338} versus εSr_{338} plot of all the intrusive rocks from the Aguablanca stock, as well as from other nearby similar plutonic massifs such as Burguillos del Cerro and Brovales, where values of $(^{87}Sr/^{86}Sr)_{338}$ as low as 0.70459 and of εNd_{338} of -2.3 have been found by the authors (unpublished data). Available isotope compositions of Upper Precambrian and Lower-Middle Cambrian detrital sediments from the region (Nägler, 1990; Schäfer, 1990; unpublished data) have been included for comparison. All the intrusives fall in the domain of supracrustal isotope compositions (e.g., Dickin, 1995). A hyperbolic regression curve can be roughly fitted to the igneous rocks and extends into the field of the sedimentary rocks. Since mixing of two end members produces a hyperbolic trend in εNd_{338}–εSr_{338} coordinates, Fig. 4 suggests that the Sr- and Nd-isotope composition of Variscan magmas in the OMZ might result from the mixing of an upper-crustal component with a primitive parental magma. In the absence of rocks of primitive composition—no earlier dykes of basic composition have been recognized—and because the mixing trend extends into the mantle-array region of the εNd_{338}–εSr_{338} plot (Fig. 4), we can argue that the parental magma was probably a basalt with an istopic composition between those of bulk earth (338 Ma ago) and depleted mantle.

The Sr- and Nd-isotope composition of the magmas can be explained in terms of assimilation–fractional crystallization (AFC) processes (DePaolo, 1981, 1985) involving a primitive parental magma of basaltic composition and low Rb/Sr supracrustal rocks. Fig. 5 is a $^{87}Sr/^{86}Sr$ versus Rb/Sr plot of the Santa Olalla igneous rocks. Two groups can be envisaged in this plot, one represented by gabbronorites and norites (PG rocks) that plot on or close to a mixing-line between a hypotetical primitive magma with the Sr-isotope signature of a Middle Cambrian basalt from the area (sample CEM-113, Table 2), and two low-Rb/Sr ratio metasediments (DC-4, Table 2; MON-4, from Nägler, 1990). The second group is represented instead by the main igneous sequence rocks, which show a large range of Rb/Sr values at an almost uniform Sr-isotope composition (most rocks between 0.7092 and 0.7095.

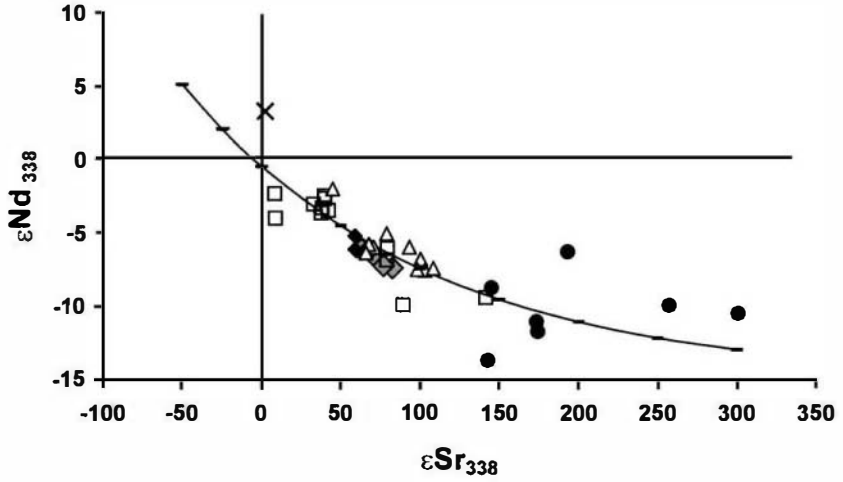

Fig. 4. εNd_{338} vs. εSr_{338} diagram of significant rocks of the Monesterio Antiform. Diamonds: Aguablanca stock (black = PG rocks; grey = diorites); squares: Burguillos Complex; triangles: Brovales Complex; dots: Metasediments; cross: Cambrian volcanic rock from the area (CEM-114).

Early crystallization of pyroxene and olivine in a deep magma chamber, accompanied by assimilation of radiogenically evolved crustal material, could have led to the evolution from the $^{87}Sr/^{86}Sr$ initial compositions shown by the cumulates to those of the main igneous sequence rocks (DePaolo, 1981, 1985). Moreover, the relatively uniform Sr-isotope composition of the latter (diorite–tonalite–monzogranite), strongly independent of the Rb/Sr ratios (0.05–0.53), can be explained by further fractional crystal-

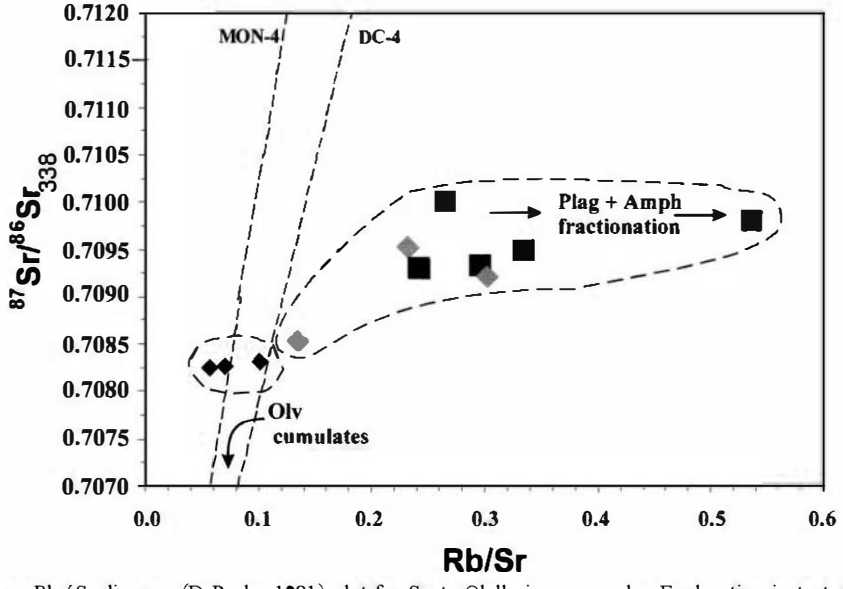

Fig. 5. $^{87}Sr/^{86}Sr_{338}$ vs. Rb/Sr diagram (DePaolo, 1981) plot for Santa Olalla igneous rocks. Explanation in text. Squares: Main Santa Olalla pluton. Diamonds: Aguablanca stock (black = PG rocks; grey = diorites).

lization of plagioclase and amphibole at lower pressures (DePaolo, 1981). The Nd-isotope composition of the main igneous sequence rocks, which is also very uniform (εNd_{338} from -6.0 to -7.5), was probably controlled by amphibole fractional crystallization. Plagioclase and amphibole have high crystal-melt partition coefficients for Sr and Nd, respectively. Simultaneous low-pressure (<2 kb) fractional crystallization of plagioclase and, to a lesser extent, of amphibole could also account for the low Eu negative anomaly and the increasing content of total REE from diorites through monzogranites (e.g., Gromet and Silver, 1987).

The isotopic homogeneity of the main igneous sequence rocks does not support the magma-mixing hypothesis invoked by Bateman et al. (1992) to explain the tonalites and biotite-amphibole diorites. In their hypothesis, tonalites and diorites resulted from the mixing of two non-consanguineous magmas, a cordierite-bearing S-type magma and a somewhat fractionated pyroxene gabbro.

Magmas with $^{87}Sr/^{86}Sr$ initial signatures lower than 0.708 have not been found in the Aguablanca Stock, probably because earlier cumulates, richer in olivine and clinopyroxene (as expected from moderate pressure fractional crystallization; see Presnall, 1999), were left behind during magma ascent from the deep magma chamber to the final emplacement level. The recent discovery of enclaves of altered serpentinized olivine-rich rocks and clinopyroxenites in the ore-rich breccia supports this interpretation.

6.3. *Constraints on the source and evolution of the ore*

The $\delta^{34}S$ values of the ore sulphides are much higher than those typical of juvenile sulphur (0 ± 3‰; Ohmoto, 1986). However, they are close to the upper end of the $\delta^{34}S$ values of igneous rocks with a large crustal component (-1‰ to $+7$‰; Sasaki and Ishihara, 1979; Matthäi et al., 1995). Although no isotope data are available from OMZ slates, sulphide mineralization hosted by Upper Precambrian to Lower Palaeozoic slates in the northern Iberian Massif show $\delta^{34}S$ values between $+7$‰ and $+21$‰ (Tornos et al., 1996). These values are consistent with bacterial sulphate reduction. In consequence, we think that the sulphur in the Aguablanca ore evidences a contribution from crustal sulphur. Sulphur contents in most OMZ supracrustal rocks are low (<50 ppm); however, Upper Precambrian slates, which are abundant in the area and probably increase with depth, are S-rich (1091 ppm) (Nägler, 1990; Schäfer, 1990). A few preliminary lead isotope data on the massive pyrrohtite indicate that the lead mostly derived from an U-rich source (values of $\mu(=^{238}U/^{204}Pb)$ are high, in the range 9.6–9.8) (Tornos et al., 1998). The data plot well above the mantle reference line but close to the average crustal curves and the expected isotopic evolution of the nearby Precambrian sediments. This is consistent with most of the lead being derived from the assimilation/leaching of regional metasediments and reinforce the hypothesis of crustal assimilation.

Assimilation of crust or crustally derived sulphur into sulphide undersaturated magmas rising from the mantle has been invoked for many well-known anorogenic giant Cu–Ni sulphide deposits of the komatiite, Duluth-type or mafic–ultramafic layered intrusions, on the basis of stable isotope geochemistry or, more recently, Re–Os systematics (see Lambert et al., 1998 for a summary). Assimilation of supracrustal pelitic material has been specifically invoked in the case of the Duluth-type Cu–Ni ore (Ripley and Al-Jassar, 1987; Acuri et al., 1998) and more recently in the Voysey's Bay Ni–Cu–Co deposit (Li and Naldrett, 2000). In the latter case, primitive troctolite-gabbro magma reacted extensively with regional gneiss that shows evidence of partial melting.

The solubility of sulphur in basic magmas is very low (Haughton et al., 1974; Ohmoto, 1986). Exsolution of S-rich liquid from the contaminated magma probably took place as a consequence of AFC processes (either assimilation of a silica-rich fraction or sulphur contamination or both), accompanied by either decreasing temperature, increasing oxygen fugacity or a combination of both (for a discussion on the role of these variables on sulphide solubility, see Naldrett, 1989b).

6.4. *Geodynamic scenario of magmatism and emplacement history*

The probable age of the Santa Olalla plutonic complex proposed above (circa 338 Ma), is close to

the beginning of type-A oblique subduction of the SPZ under the OMZ (Silva et al., 1990). Transpression in the SW Iberian margin was accompanied by faulting, both reverse and strike-slip (Sanderson et al., 1991), and high-K calc-alkaline magmatism along the margin of the OMZ. Northward subduction of an oceanic lithosphere has long been invoked to explain this magmatism in the OMZ (e.g., Quesada et al., 1994). In consequence, the Aguablanca Ni–Cu ore must be classified as synorogenic in the sense of Naldrett (1989a).

Most synorogenic Cu–Ni ore deposits are hosted by Alaskan-type mafic–ultramafic plutonic complexes (e.g., Naldrett, 1989a), which show both similarities and differences with the Santa Olalla plutonic complex. In fact, they form small-zoned intrusions in convergent plate-margin settings (Himmelberg and Loney, 1995). However, Alaskan-type complexes are formed of mafic and ultramafic cumulates, particularly dunites, clinopyroxene peridotites, clinopyroxenite, hornblendite and orthopyroxene-bearing gabbros, derived from fractionation of a primitive subalkaline basaltic magma (Himmelberg et al., 1986; Himmelberg and Loney, 1995; Tistl et al., 1994). Some of these rock-types are either missing or found as minor enclaves in the Santa Olalla plutonic complex.

Wyborn (1992) has suggested that the Fifield (Australia) Alaskan-type intrusions were mid-crustal chambers that were probably the source of shosonitic volcanic rocks of the Lachlan Fold Belt. High-K calc-alkaline rocks and the shosonitic rock series are commonly associated in ensialic mobile belts (e.g., Wilson, 1989). Thus, a link between the Alaskan-type magmatic Cu–Ni sulphides and the special case represented by the Aguablanca ore, hosted by high-K calc-alkaline rocks, although conjectural, remains a possibility.

We envisage the intrusion as a two-step process. Parental basaltic magma first ponded at some unknown depth within the upper continental crust, where AFC processes began involving S-bearing metasediments. Contact melting probably played a role in this process, as evidenced by the presence of restitic peraluminous xenoliths in the Aguablanca mafic–ultramafic rocks. Sinking of early formed pyroxenes and olivine then started, along with the formation of a sulphide magma that, because of its high density, also sank. Subsequently, cumulates, together with sulphide magma and residual, partially crystallized magma, were sequentially tapped to the final emplacement level at a shallow depth (2–4 km). Fractional crystallization of plagioclase and amphibole began at a depth corresponding to circa 2 kb, giving rise to the main igneous sequence magmas (diorite → tonalite → monzogranites) that were intruded with a reverse gradational zonal pattern. Transpressive structures such as reverse and strike-slip faults, particularly the nearby Cherneca Fault, probably played a significant role in driving magma ascent. Due to the small size of the mineralized breccia pipe, fast ascent would been necessary to keep sulphide magma well above solidus temperatures. Fast sulphide magma ascent is in fact suggested by breccia textures in the pipe. Dilational structures related to a major fault tapping the magmatic chamber at depth could have offered suitable pathways for a quick magma ascent. The lens shape and subvertical disposition of the pipe argue in favour of this process.

Acknowledgements

The radiogenic isotope (Sr and Nd) work was carried out by C.G. at the NERC Isotope Geosciences Laboratory (Keyworth, UK). We acknowledge the laboratory advice by Dr. Robert Pankhurst of the British Antarctic Survey. The final version of this text was reviewed by Christine Laurin. Financial support was provided in part by Spanish grants AMB92-0918-C02-01 and DGES96-0135. This paper is a contribution of the IGCP 427 project.

References

Arcuri, T., Ripley, E.M., Hauck, S.A., 1998. Sulphur and oxigen isotope studies of the interaction between pelitic xenoliths and basaltic magma at the Babbitt and Serpentine Cu–Ni deposits, Duluth Complex, Minnesota. Econ. Geol. 93, 1063–1075.

Bateman, R., Martín, M.P., Castro, A., 1992. Mixing of cordierite granitoid and pyroxene gabbro, and fractionation, in the Santa Olalla tonalite (Andalucia). Lithos 28, 111–131.

Börg, S.G., De Paolo, D.J., Smith, B.M., 1990. Isotopic structure and tectonics of the central Transantarctic Mountains. J. Geophys. Res. 95, 6647–6667.

Casquet, C., 1980. Fenomenos de endomorfismo, metamorfismo y metasomatismo de contacto en los mármoles de Rivera de Cala (Sierra Morena). Doctoral Thesis, Madrid, Spain, Complutense University, 295 pp.

Casquet, C., Galindo, C., Darbyshire, D.P.F., Noble, S.R., Tornos, F., 1998. Fe-U-REE mineralization at Mina Monchi, Burguillos del Cerro, SW Spain: age and isotope (U–Pb, Rb–Sr and Sm–Nd) constraints on the evolution of the ores. GAC-MAC-APGGQ, Quebec '98 Conference, Abstract Vol., v. 23: A-28.

Casquet, C., Eguiluz, L., Galindo, C., Tornos, F., Velasco, F., 1999. The Aguablanca Cu–Ni(PGE) intraplutonic ore deposit (Extremadura, Spain). Isotope (Sr, Nd, S) constraints on the source and evolution of magmas and sulphides. Geogaceta 24, 71–72.

Dallmeyer, R.D., García-Casquero, J.L., Quesada, C., 1995. $^{40}Ar/^{39}Ar$ mineral age constraints on the emplacement of the Burguillos del Cerro Igneous Complex (Ossa Morena Zone, SW Iberia). Bol. Geol. Min. 106, 203–214.

DePaolo, D.J., 1981. Trace element and isotopic effects of combined wallrock assimilation and fractional crystallization. Earth Planet. Sci. Lett. 53, 189–202.

DePaolo, D.J., 1985. Isotopic studies of processes in mafic magma chambers: I. The Kiglapait intrusion, Labrador. J. Petrol. 26, 925–951.

Dickin, A.P., 1995. Radiogenic Isotope Geology. Cambridge Univ. Press, Cambridge, 452 pp.

Gromet, L.P., Silver, L.T., 1987. REE variations across the Peninsular Ranges batholith: implications for batholithic petrogenesis and crustal growth in magmatic arcs. J. Petrol. 28, 75–125.

Haughton, D.R., Roeder, P.L., Skinner, B.J., 1974. Solubility of sulphur in basic magmas. Econ. Geol. 69, 451–467.

Himmelberg, G.L., Loney, R.A., 1995. Characteristics and petrogenesis of Alaskan-type ultramafic–mafic intrusions, Southestern Alaska. U.S. Geol. Surv. Prof. Pap. 1564, 47 pp.

Himmelberg, G.R., Loney, R.A., Craig, J.T., 1986. Petrogenesis of the ultramafic complex at the Blashke Islands, southeastern Alaska. U.S. Geol. Surv. Bull. 1662, 14 pp.

Jacobsen, S.B., Wasserburg, G.J., 1980. Sm–Nd isotopic evolution of chondrites. Earth Planet. Sci. Lett. 50, 139–155.

Lambert, D.D., Foster, J.G., Frick, L.R., Ripley, E.M., Zientek, M.L., 1998. Geodynamics of magmatic Cu–Ni–PGE sulphide deposits: new insights from the Re–Os systems. Econ. Geol. 93, 121–137.

Li, C., Naldrett, A., 2000. Melting reactions of gneissic inclusions with enclosing magma at Voysey's Bay, Labrador, Canada: implications with respect to ore genesis. Econ. Geol. 95, 801–814.

Lunar, R., Ortega, L., Sierra, J., Garcia Palomero, F., Moreno, T., Prichard, H., 1997. Ni–Cu (PGM) mineralization associated with mafic and ultramafic rocks: the recently discovered Aguablanca ore deposit, SW Spain. In: Papunen, H. (Ed.), Mineral Deposits. Balkema, Rotterdam, pp. 463–466.

Matthäi, S.K., Henley, R.W., Heinrich, A., 1995. Gold precipitation by fluid mixing in bedding-parallel fractures near carbonaceous slates at the Cosmopolitan Howley gold deposit, Northern Australia. Econ. Geol. 90, 2123–2142.

Nägler, T., 1990. Sm–Nd, Rb–Sr and common lead isotope geochemistry on fine-grained sediments of the Iberian Massif. Doctoral Thesis, Zurich, Switzerland, ETH Diss., No.9245, 141 pp.

Naldrett, A.J., 1989a. Introduction: magmatic deposits associated with mafic rocks. Rev. Econ. Geol. 4, 1–4.

Naldrett, A.J., 1989b. Sulphide melts: crystallization temperatures, solubilities in silicate melts, and Fe, Ni, and Cu partitioning between basaltic magmas and olivine. Rev. Econ. Geol. 4, 5–20.

Ohmoto, H., 1986. Stable isotope geochemistry of ore deposits. Rev. Mineral. 16, 401–556.

Ortega, L., Moreno, T., Lunar, R., Prichard, H., Sierra, J., Bomati, O., Fisher, P., Garcia Palomero, F., 1999. Minerales del grupo del platino y fases asociadas en el depósito de Ni–Cu–EGP) de Aguablanca, SO España. Geogaceta 25, 155–158.

Quesada, C., Fonseca, P.E., Munhá, P.E., Oliveira, J.M., Ribeiro, A., 1994. The Beja-Acebuches Ophiolite (Southern Iberia Variscan foldbelt): geological characterization and geodynamic significance. Bol. Geol. Min. 105, 3–49.

Presnall, D.C., 1999. Effect of pressure on the fractional crystallization of basaltic magma. In: Fei, Y., Bertka, M., Mysen, B.O. (Eds.), Mantle Petrology: Field Observations and High Pressure Experimentation: A Tribute to Francis R. Boyd. Geochem. Soc., Spec. Publ. 6, pp. 209–224.

Ripley, E.M., Al Jassar, T.J., 1987. Sulphur and oxigen isotope studies of melt–country rock interaction, Babbitt Cu–Ni deposit; Duluth Complex, Minnesota. Econ. Geol. 82, 87–107.

Rollinson, H., 1993. Using Geochemical Data: Evaluation, Presentation, Interpretation. Longman, New York, 352 pp.

Sanderson, D.J., Roberts, S., McGowan, A., Gumiel, P., 1991. Hercynian transpressional tectonics at the southern margin of the Central Iberian Zone, west Spain. J. Geol. Soc. (London) 148, 893–898.

Sasaki, A., Isihara, S., 1979. Sulphur isotopic composition of the magnetite-series and ilmenite-series granitoids in Japan. Contrib. Mineral. Petrol. 68, 107–115.

Schäfer, H.J., 1990. Geochronological Investigations in the Ossa-Morena Zone, SW Spain. Doctoral Thesis, Zurich, Switzerland, ETH Diss., No.9246, 153 pp.

Silva, J.B., Oliveira, J.T., Ribeiro, A., 1990. South Portuguese Zone: stratigraphy and synsedimentary tectonism. In: Dallmeyer, R.D., Martinez García, E. (Eds.), Pre-Mesozoic Geology of Iberia. Springer-Verlag, Berlin, pp. 348–362.

Steiger, R.H., Jäger, E., 1977. Subcomission on geochronology: convention on the use of decay constant in geo- and cosmochronology. Earth Planet. Sci. Lett. 36, 359–362.

Taylor, S.R., McLennan, S.M., 1981. The composition and evolution of the continental crust: rare earth element evidence from sedimentary rocks. Philos. Trans. R. Soc. London A301, 381–399.

Thompson, R.N., 1982. Magmatism of the British Tertiary volcanic province. Scott. J. Geol. 18, 49–107.

Tistl, M., Burgath, K.P., Hoehndorf, A., Kreuzer, H., Munoz, R., Salinas, R., 1994. Origin and emplacement of tertiary ultramafic complexes in Northwest Colombia; evidence from geochemistry and K–Ar, Sm–Nd and Rb–Sr isotopes. Earth Planet. Sci. Lett. 126, 41–59.

Tornos, F., Ribera, F., Shepherd, T.J., Spiro, B., 1996. The geologic and metallogenetic setting of stratabound carbonate-hosted Zn–Pb mineralizations in the West Asturian Leonese Zone (NW Spain). Miner. Deposita 31, 27–40.

Tornos, F., Chiaradia, M., Fontboté, L., 1998. La geoquímica isotópica del plomo en las mineralizaciones de la Zona de Ossa Morena (ZOM): implicaciones metalogenéticas y geotectónicas. Bol. Soc. Esp. Min. 21-A, 206–207.

Tornos, F., Casquet, C., Galindo, C., Canales, A., Velasco, F., 1999. The genesis of the Variscan ultramafic-hosted magmatic Cu–Ni deposit of Aguablanca, SW Spain. In: Stanley, C.G., et al., (Eds.), Mineral Deposits: Processes to Processing. Balkema, Rotterdam, pp. 795–798.

Velasco, F., 1976. Mineralogía y metalogenia de los skarns de Santa Olalla (Huelva). Umpublished Doctoral Thesis, Bilbao, Spain, University of Bilbao, 290 pp.

Wilson, M. et al., 1989. Igneous Petrogenesis. A Global Tectonic Approach. Unwin Hyman, London, 466 pp.

Wyborn, D., 1992. The tectonic significance of Ordovician magmatism in the eastern Lachlan Fold Belt. Tectonophysics 214, 177–192.